

# **SANDIA REPORT**

SAND2005-6252

Unlimited Release

Printed November 2005

## **LDRD Final Report on Adaptive-Responsive Nanostructures for Sensing Applications**

Zhongchun Wang, Craig J. Medforth, Frank van Swol, John A. Shelnett

Prepared by  
Sandia National Laboratories  
Albuquerque, New Mexico 87185 and Livermore, California 94550

Sandia is a multiprogram laboratory operated by Sandia Corporation, a Lockheed Martin Company, for the United States Department of Energy's National Nuclear Security Administration under Contract DE-AC04-94AL85000.

Approved for public release; further dissemination unlimited.



Issued by Sandia National Laboratories, operated for the United States Department of Energy by Sandia Corporation.

**NOTICE:** This report was prepared as an account of work sponsored by an agency of the United States Government. Neither the United States Government, nor any agency thereof, nor any of their employees, nor any of their contractors, subcontractors, or their employees, make any warranty, express or implied, or assume any legal liability or responsibility for the accuracy, completeness, or usefulness of any information, apparatus, product, or process disclosed, or represent that its use would not infringe privately owned rights. Reference herein to any specific commercial product, process, or service by trade name, trademark, manufacturer, or otherwise, does not necessarily constitute or imply its endorsement, recommendation, or favoring by the United States Government, any agency thereof, or any of their contractors or subcontractors. The views and opinions expressed herein do not necessarily state or reflect those of the United States Government, any agency thereof, or any of their contractors.

Printed in the United States of America. This report has been reproduced directly from the best available copy.

Available to DOE and DOE contractors from  
U.S. Department of Energy  
Office of Scientific and Technical Information  
P.O. Box 62  
Oak Ridge, TN 37831

Telephone: (865)576-8401  
Facsimile: (865)576-5728  
E-Mail: [reports@adonis.osti.gov](mailto:reports@adonis.osti.gov)  
Online ordering: <http://www.osti.gov/bridge>

Available to the public from  
U.S. Department of Commerce  
National Technical Information Service  
5285 Port Royal Rd  
Springfield, VA 22161

Telephone: (800)553-6847  
Facsimile: (703)605-6900  
E-Mail: [orders@ntis.fedworld.gov](mailto:orders@ntis.fedworld.gov)  
Online order: <http://www.ntis.gov/help/ordermethods.asp?loc=7-4-0#online>



# LDRD Final Report on Adaptive-Responsive Nanostructures for Sensing Applications

Zhonchun Wang, Craig J. Medforth,  
Frank van Swol, John A. Shelnett  
Surface Interface Sciences  
Sandia National Laboratories  
PO Box 5800  
Albuquerque, NM 87185-1349

## Abstract

Functional organic nanostructures such as well-formed tubes or fibers that can easily be fabricated into electronic and photonic devices are needed in many applications. Especially desirable from a national security standpoint are nanostructures that have enhanced sensitivity for the detection of chemicals and biological (CB) agents and other environmental stimuli. We recently discovered the first class of highly responsive and adaptive porphyrin-based nanostructures that may satisfy these requirements. These novel porphyrin nanostructures, which are formed by ionic self-assembly of two oppositely charged porphyrins, may function as conductors, semiconductors, or photoconductors, and they have additional properties that make them suitable for device fabrication (e.g., as ultrasensitive colorimetric CB microsensors). Preliminary studies with porphyrin nanotubes have shown that these nanostructures have novel optical and electronic properties, including strong resonant light scattering, quenched fluorescence, and electrical conductivity. In addition, they are photochemically active and capable of light-harvesting and photosynthesis; they may also have nonlinear optical properties. Remarkably, the nanotubes and potentially other porphyrin nanostructure are mechanically responsive and adaptive (e.g., the rigidity of the micrometers-long nanotubes is altered by light, ultrasound, or chemicals) and they self-heal upon removal the environmental stimulus. Given the tremendous degree of structural variation possible in the porphyrin subunits, additional types of nanostructures and greater control over their morphology can be anticipated. Molecular modification also provides a means of controlling their electronic, photonic, and other functional properties. In this work, we have greatly broadened the range of ionic porphyrin nanostructures that can be made, and determined the optical and responsivity properties of the nanotubes and other porphyrin nanostructures. We have also explored means for controlling their morphology, size, and placement on surfaces. The research proposed will lay the groundwork for the use of these remarkable porphyrin nanostructures in micro- and nanoscale devices, by providing a more detailed understanding of their molecular structure and the factors that control their structural, photophysical, and chemical properties.



## Introduction

Functional nanostructures that can easily be fabricated into electronic and photonic devices are a highly desirable goal, especially if such materials can be used to enhance detection sensitivities for chemicals and biological (CB) agents. Recently, we discovered a family of highly responsive and adaptive nanostructures composed of ionic materials made from two oppositely charged porphyrins, which have properties that make them suitable for device fabrication.<sup>1,2</sup> Preliminary studies have shown that the first members of this family of porphyrin nanostructures, porphyrin nanotubes, have novel optical and electronic properties and that they are photochemically active and capable of light-harvesting and photosynthesis. The nanotubes are mechanically responsive and adaptive, with the rigidity of the nanotubes being reversibly altered by light, ultrasound, or chemicals. These properties make the nanotubes potentially useful as highly specific and sensitive detectors (transducers). Moreover, given the tremendous degree of structural variation possible in the porphyrin subunits, the synthesis of additional types of nanostructures with controlled morphologies and electronic, photonic, and other functional properties can be anticipated. Most importantly, the micrometers-long nanotubes and other linear nanostructures are suitable for fabrication into microsensors for CB agents and might provide greatly enhanced responsivity.

Colorimetric porphyrin arrays have already been demonstrated in ultrasensitive CB detectors;<sup>3</sup> the ability now to assemble these porphyrins into well-formed responsive nanostructures will enable significantly enhanced capabilities compared to these earlier devices. We propose to establish the range of ionic porphyrin nanostructures that can be made and to determine their electrical, optical, and responsivity properties. We will explore means for controlling their morphology, size, and placement on surfaces. We will also investigate their unusual photonic, electronic, and mechanical-switching properties, and evaluate their potential use in CB sensors and other applications.

The key obstacles to the implementation of these porphyrin nanostructures in useful device configurations are the lack of a detailed understanding of their structure and the lack of sufficient knowledge concerning the factors that control their structure and physical and chemical properties. The research proposed will lay the groundwork for the use of these remarkable nanostructures as CB sensors and in other micro- and nanoscale devices.

Self-assembled materials with well-defined shapes and dimensions are of great current interest,<sup>4</sup> and applications of the porphyrin-based nanomaterials such as the nanotubes can be foreseen in many applications such as electronics, photonics, light-energy conversion, and catalysis. Similarly, carbon nanotubes (CNTs) are a well-known nanomaterials that are being employed in these application, but CNTs have shortcomings including difficulties in controlling their high temperature synthesis (and thus their electronic properties) and their limited range of functional capabilities. Interestingly, some researchers are attempting to add new functionality (*e.g.*, photoconductivity) to CNTs by attaching porphyrins (phthalocyanines) to their surfaces<sup>5</sup> or by encapsulating porphyrins within CNTs.<sup>6</sup> Instead, we thought why not simply self-assemble the porphyrins themselves into nanotubes?

Porphyrins are attractive building blocks for functional nanostructures because of their desirable electronic, optical, and catalytic properties, but previously their use has been limited by the scarcity of porphyrin nanostructures with shapes suitable for incorporation into devices. A few porphyrin nanostructures have been prepared on surfaces including fibers, rods, sheets, and stripes,<sup>7-10</sup> but more robust porphyrin nanostructures with useful and well-defined shapes are needed. Porphyrins and other tetrapyrroles (phthalocyanines, chlorophylls) are well-known to form aggregates with useful optical and electronic properties.<sup>11</sup>

Synthetic porphyrins such as the dication of meso-tetrakis(4-sulfonatophenyl)porphyrin ( $H_4TPPS_4^{2-}$ ) shown in Fig. 1 form nanoscale aggregates composed of off-set stacked molecules (*J*-aggregates) in aqueous solution at pH 1 or at high ionic strength. These *J*-aggregates display novel optical properties arising from the alignment and coherent coupling of the transition dipoles of the stacked porphyrins. Essentially, the coupled molecules scatter light by acting together as a single large molecule. These  $H_4TPPS_4^{2-}$  aggregates sometimes form useful nanostructures on surfaces,<sup>9,10</sup> but porphyrin self-aggregates are more typically in the form of sheets or fractal objects that are not easily incorporated into devices. We describe a new technical approach based on ionic self-assembly for making well-formed free-standing porphyrin nanostructures that may be suitable for integration into a range of devices.

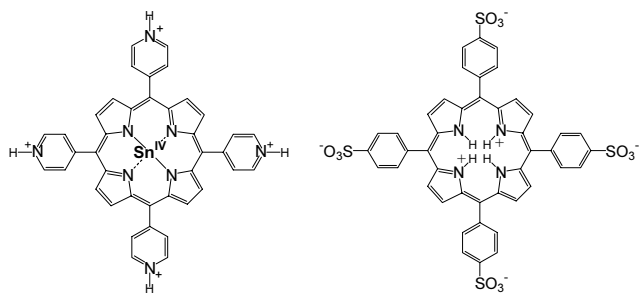


**Fig. 1.** Porphyrins used in making the porphyrin nanotubes.  $Sn(IV)TPyP^{2+}$  (left) and  $H_4TPPS_4^{2-}$  (right) The tin porphyrin will usually have axial ligands bound to the metal above and below the porphyrin plane.

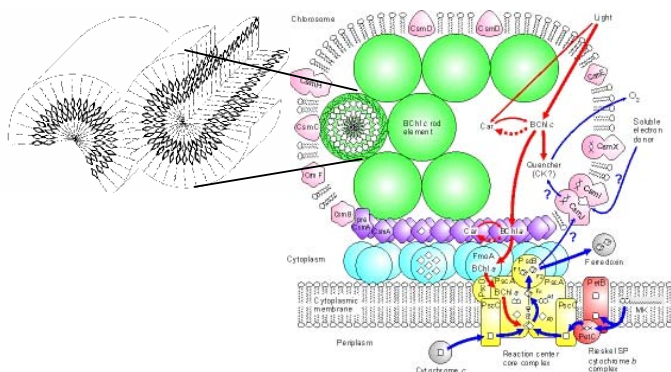


**Fig. 2.** Chlorosomes and chlorosomal rods. Light-harvesting is done by the chlorosomal rods, which are composed of self-assembled bacteriochlorophyll molecules.

In nature, porphyrins, such as chlorophylls and hemes, perform the essential light harvesting and energy-transduction and utilization functions upon which all life is based. The porphyrins that perform these energy- and electron-transfer tasks are self-organized in nanoscale biological superstructures. An interesting example of these biological nanostructures is the light-harvesting rods of the chlorosomes of green-sulfur bacteria, which are composed of chlorophyll aggregates<sup>12</sup> as illustrated in Fig. 2. We have recently discovered similar porphyrin nanostructures, including nanotubes that mimic these biological structures. The tubes are formed by ionic self-assembly of two oppositely charged porphyrins in aqueous solution and represent a new class of porphyrin nanostructures. Importantly, the molecular building blocks can be altered to control their morphology and properties and to produce other new nanostructures. The nanotubes are well-formed, robust, hollow structures that exhibit interesting electronic and optical properties such as intense resonance light scattering. They are also responsive and adaptive to environmental

stimuli such as chemicals and light. In addition, the nanotubes are photocatalytic, capable of reducing metal ions that deposit selectively onto tube surfaces to form novel nanotube-metal composite systems.

In this work, we have exploited this discovery by exploring what types of porphyrin nanostructures can be made and by determining how their structure and properties might be controlled to facilitate their use in integrated devices, especially chemical sensors. Our research advances the aim of the integration of biological and biomimetic nanostructures into microelectronic devices, possibly leading to ultrasensitive sensors for chemical and biological agents for counterterrorism and warfar. In addition, the porphyrin nanotubes and related porphyrin nanostructures hold promise for use in nanoscale electronic and photonic devices such as reconfigurable conductors, photonic lattice elements, alterable nanofluidic channels, and nanomechanical elements. Potentially, they provide a new suite of components for the fabrication of functional nanosystems. As catalytic nanostructures, they may also impact energy security and the implementation of a hydrogen economy based on solar energy.

## Accomplishments

Proposed tasks were (1) to investigate of the conditions under which porphyrin nanostructures form, with the goals of better controlling their uniformity and morphology and potentially producing entirely new structures; (2) to obtain precise synthetic control over porphyrin nanostructure and functional properties; and (3) to synthesize additional types of nanostructures by varying the substituent groups attached to the porphyrin, the metal in the porphyrin core, and the axial ligands of the tectons. All of these goals were met and the resulting porphyrin nanostructures were characterized by electron microscopy. We have also extensively explored the novel optical and electronic properties afforded by several of the new porphyrin nanostructures. In many cases the molecular structure of the ionic solid composed of the porphyrins remains a mystery, but general rules about the composition and the porphyrin packing arrangement have been determined using experimental techniques. In addition, a Monte-Carlo computational technique has been developed to handle the self-assembly of parallopipeds with charges near the corners and at its center. This simulation technique well models the porphyrin volume and intermolecular interactions and is now be available for future studies of these unique ionic nanostructures. Further studies of photosynthetic H<sub>2</sub> evolution by platinized nanotubes were also accomplished. Finally, we also evaluated the interactions of the nanostructures with various chemicals and the potential for producing arrays of porphyrin nanostructures in CB microsensors.

Our novel approach to synthesizing porphyrin nanostructures is based on ionic self-assembly, where aggregates are formed by coupling two oppositely charged water-soluble porphyrins.<sup>1,2</sup> Ionic self-assembly relies on the strong electrostatic forces between oppositely charged porphyrin molecules (Fig. 2), together with the van der Waals, hydrogen-bonding, axial coordination, and other weak intermolecular interactions that usually contribute to non-ionic self-assembly. We have already shown that ionic self-assembly leads to well-formed porphyrin nanotubes (Fig. 3), wherein the porphyrins act as two types of charged tectonic units that cooperatively self-assemble by molecular recognition processes into the nanostructure. Most importantly, the porphyrin nanotubes produced by ionic self-assembly retain the desirable properties of porphyrin self-aggregates (*e.g.*, *J* aggregate-type electronic coupling), and they may be expected to mimic the light-harvesting and photosynthetic functions of the chlorosomal rods.

The porphyrin nanotubes that we have prepared are self-assembled by mixing aqueous solutions of two porphyrins such as those shown in Fig. 1. Typically, equal volumes of an acidified  $\text{H}_4\text{TPPS}_4^{2-}$  solution (10.5  $\mu\text{M}$ ) and a Sn(IV)-tetrakis(4-pyridyl)porphyrin ( $\text{Sn(IV)TPyP}^{2+}$ ) dichloride solution (3.5  $\mu\text{M}$ ) were mixed and left in the dark for 72 hours. Although neither of the individual porphyrins forms aggregates under these acidic solution conditions (pH 2), the mixture immediately forms colloidal aggregates and, over time, results in an abundance of the porphyrin nanotubes (>90%). Tube formation is very sensitive to solution conditions, especially pH, because it alters the charge balance. We have investigated the optimal conditions for nanostructure formation with the goal of better controlling uniformity and morphology and producing entirely new nanostructures.

The transmission electron microscope (TEM) images of the porphyrin nanotubes shown in Fig. 3 reveal that they are micrometers in length and have diameters in the range of 50-70 nm. Typically, the tube wall thickness is approximately 20 nm. The TEM image in the Inset of Fig. 3 shows that the nanotubes are hollow. The porphyrin molecules are approximately  $2 \times 2 \times 0.5$  nm, so the  $\sim 20$  nm walls must be between 10 and 40 layers of porphyrins thick. Fringes with 1.7-1.8-nm spacing at the edges of the nanotubes are seen in high resolution TEM images, probably as a result of the staining effect of the heavy sulfur and tin atoms. X-ray diffraction studies show broad lines indicating that the nanotubes are moderately crystalline. Nanorods are also observed in some TEM images and these may be collapsed tubes. We have further studied the nanostructures by electron microscopy and looked into ways of orienting the tubes on surfaces (*e.g.*, by aligning the nanotubes in arrays of nanoscale grooves on Si produced at UNM).

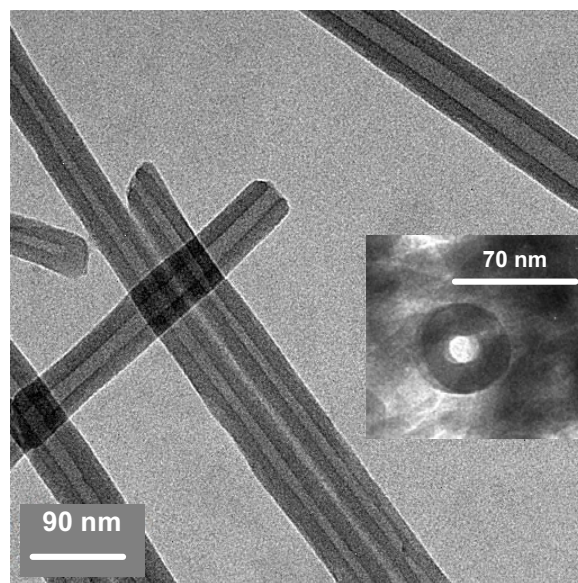


**Fig. 3.** *Transmission electron microscopy images of the porphyrin nanotubes. A group of nanotubes and Inset: a tube caught in a vertical orientation verifying that the tubes are hollow.*

The composition of the porphyrin nanotubes has been determined by UV-visible absorption spectroscopy and energy dispersive X-ray (EDX) spectroscopy. The filtered and washed nanotubes were disaggregated at pH 12 and the ratio of the porphyrins in the tubes was determined by spectral simulation, giving a ratio of 2.0-2.5 sulfonated porphyrins per tin porphyrin. EDX measurements of the S:Sn atomic ratio of tubes on TEM grids gave a similar stoichiometry. The composition of the tubes is consistent with the charges of the porphyrin species present at pH 2. Titrations monitored by UV-visible spectroscopy show that the porphyrin species present are  $\text{H}_4\text{TPPS}_4^{2-}$  and  $\text{Sn(OH)}_2\text{T(Py)}\text{P}^{4+}$  and  $\text{Sn(OH)(H}_2\text{O)T(Py)}\text{P}^{5+}$ . EDX spectra of the nanotubes showed no chlorine (from the HCl used to lower the pH), precluding the participation of chloride as counter ions, axial ligands, or salt bridges in the assembly. Water molecules might play a structural role however. As expected for a nanostructure formed by ionic self-assembly, the same ratio of porphyrins is observed in the nanotubes regardless of the initial porphyrin concentrations. The formation of the nanotubes is strongly dependent on pH (not formed at pH 1 or 3) and ionic



strength. The pH sensitivity may result partly from the equilibrium between water and hydroxide ligands on the tin(IV) ion, which alters the charge balance of the ionic tectons. We have investigated the molecular structure of the ionic solid using experimental techniques and we have developed a Monte-Carlo simulation, which can help to elucidate the porphyrin packing arrangement.

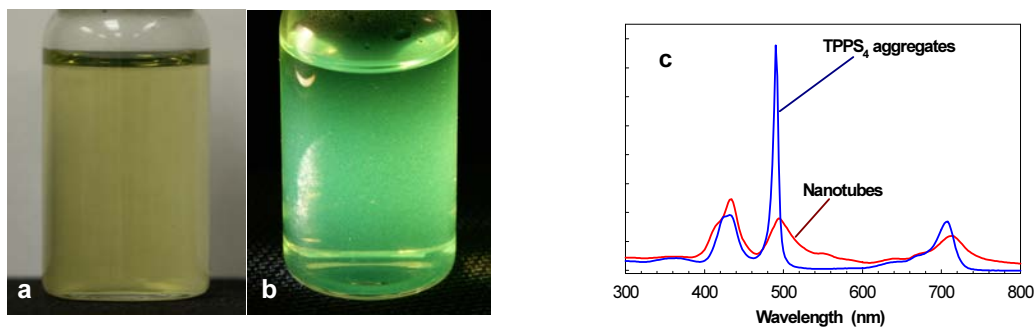


**Fig. 4.** Porphyrin nanotubes observed in transmitted light (a), observed perpendicular to intense white light, which is dominated by resonance light scattering (b), and the absorption spectra of the nanotubes and the  $H_4TPPS_4$  J-aggregates (c).

The optical spectrum of the nanotubes (Fig. 4c) consists of both absorption and resonance scattering components. The band near 490 nm is indicative of J-aggregates (as seen for  $H_4TPPS_4^{2-}$  self-aggregates). The visual effect of the resonant light scattering component is shown in Fig. 4, where the nanotubes appear light greenish yellow in transmitted light (Fig. 4a), but bright green under intense white light illumination (Fig. 4b). The width of the 490-nm band (Fig. 4c) is inversely related to the coherence length of coupling of transition dipoles, so the broadness of the band for the nanotubes indicates a coherence length that is less than the 10-20 molecules that was estimated for  $H_4TPPS_4^{2-}$ . When the nanotubes settle to the bottom of the vessel or are dried on glass or silicon surfaces, the tubes retain their brilliant green color. Strikingly, the usually strong fluorescence of the sulfonated and tin porphyrin monomers is quenched in the nanotubes. In this work, we have further characterized the novel optical and electronic properties afforded by these porphyrin nanostructures.

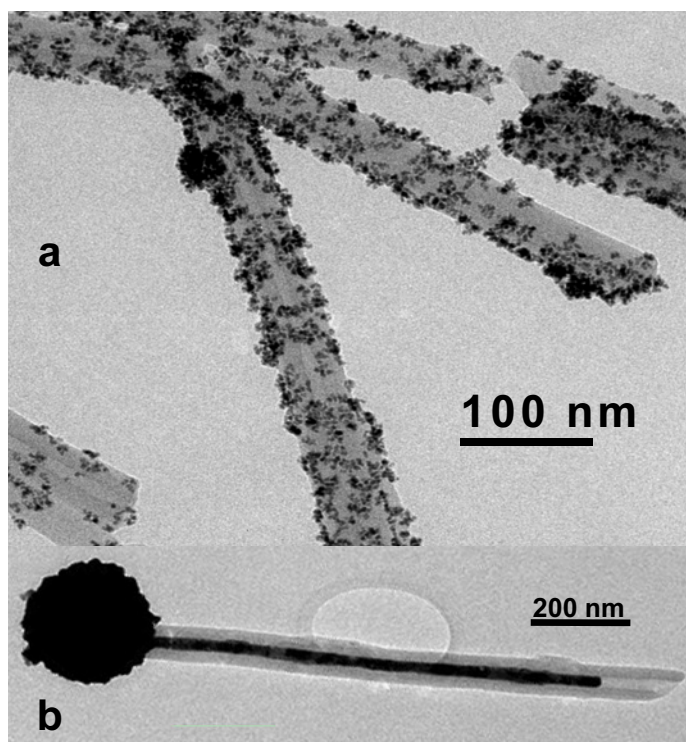


**Fig. 5.** *Platinized (a) and gilded (b) porphyrin nanotubes.*

5b). Only continuous gold wires are found, and the wires are terminated at one end of the tube with a gold nanoparticle. For the platinized nanotubes, we will determine the photosynthetic  $H_2$  evolution quantum yield. The intriguing energy- and electron-transport processes that must be at play within the tube walls to produce the gilded tubes presage good prospects for making other novel functional nanosystems—a major goal of our research.

Remarkably, the porphyrin nanotubes can serve as templates for the growth of nanotube-metal composites which might more easily be incorporated into sensor devices. By using the photocatalytic properties of the tin porphyrin contained in the nanotubes and a suitable electron donor such as ascorbic acid, metal ions can be reduced and deposited<sup>13</sup> onto the nanotube surfaces as shown in Fig. 5. Photocatalytic  $Pt^{2+}$  reduction by the tubes gives nanoparticles decorating the outer surfaces of the nanotubes (Fig. 5a). When gold(I) ions are photocatalytically reduced by the nanotubes, the gold metal is deposited exclusively within the hollow interior of the nanotubes as continuous gold nanowires (Fig.

We have shown that the dimensions of the nanotubes can be varied by altering the molecular structure of the porphyrins used. For example, altering the pyridine-substituted porphyrin by switching the position of the nitrogen atom in the pyridine ring from the 4- to 3-position (Fig. 6, Inset) produces nanotubes with approximately half the diameter of those formed by the 4-pyridyl porphyrin (Fig. 3). The TEM image of one of the nanotubes formed by the 3-pyridyl porphyrin is shown in Fig. 6. Further, by varying the substituent groups attached to the porphyrin (as just described), the metal contained in the porphyrin core, and the nature of the axial ligands, we have obtained more precise synthetic control over the nanotube structures and their functional properties.

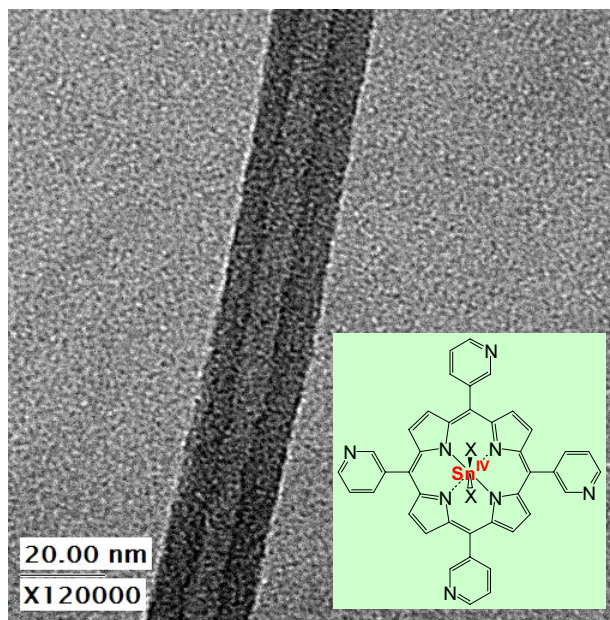


**Fig. 6.** TEM images of a porphyrin nanotube formed by ionic self-assembly of Sn tetra(3-pyridyl)porphyrin and tetra(4-sulfonatophenyl)porphyrin diacid.

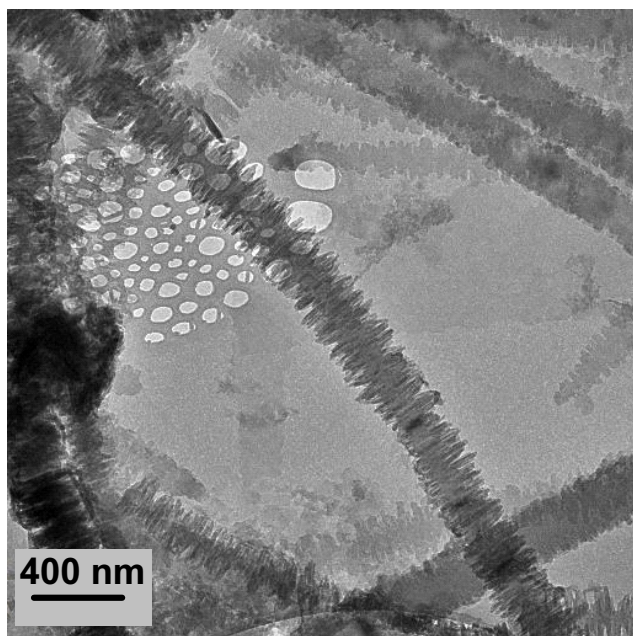


**Fig. 7.** Complex porphyrin nanostructure formed by ionic self-assembly of porphyrins.

More drastic variation of the molecular porphyrin structure leads to the complex porphyrin nanostructures such as those shown in Figs. 7-10. We have produced a wide variety of these additional types of porphyrin-based nanostructures such as the “string of firecracker” structures shown in Fig. 7 for possible use in chemical and biological sensing applications. New, more promising porphyrin nanostructure for sensor applications are shown in Figs. 8-10 and Fig. 12.



Fig. 8 shows microscale porphyrin structures resembling four-leaf clovers complete with a central stalk and the veins of the leaves. These porphyrin ‘micro-clovers’

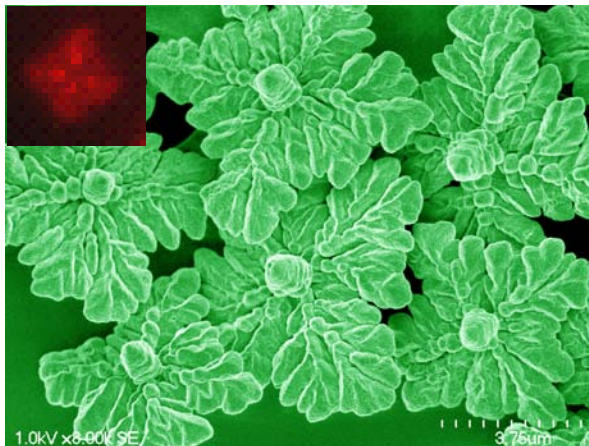


**Fig. 8.** Porphyrin ‘micro-clovers’ formed by ionic self-assembly of two porphyrins, one of which is photocatalytic—*Sn* tetra(sulfonatophenyl)porphyrin (*SnTPPS*<sub>4</sub>). Inset: Fluorescence micrograph showing regio-selective emission from one of the ‘clovers’.

have interesting optical properties that may make them suitable for sensor and other applications. Unlike the porphyrin nanotubes, fluorescence of the tectons is not quenched and they do not show significant resonance scattering. Confocal microscope images show that their fluorescence comes mainly from the ‘spines’ of the leaves when viewed in the orientation shown in the Inset of Fig. 8. Very little emission comes from the central stalk of the clover when viewed in this orientation, indicating regio-specific fluorescence from these porphyrin structures. The microclover should also exhibit photocatalytic activity since one of the porphyrin tectons is a tin porphyrin (the other is a free base porphyrin).

**Fig. 9.** Porphyrin microtubes formed by ionic self-assembly of two porphyrins, *SnTPPS*<sub>4</sub> and a free base porphyrin, in the presence of phenylalanine. Top: white light microscope image. Bottom: Fluorescence micrograph. Inset: TEM image of the microtubes.

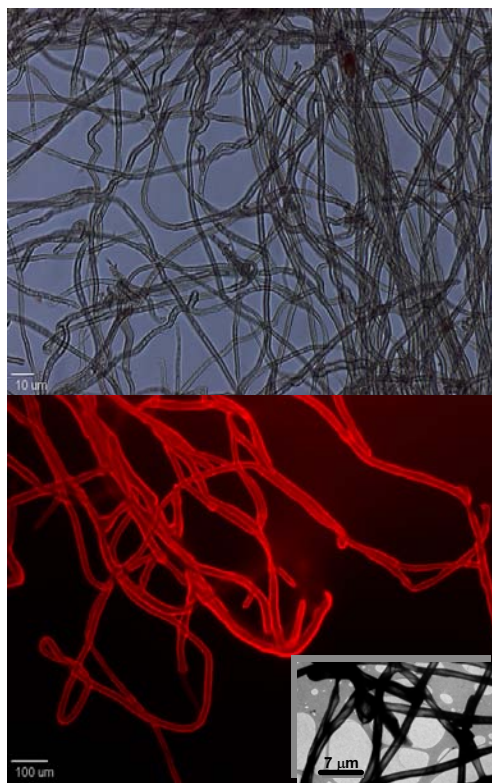
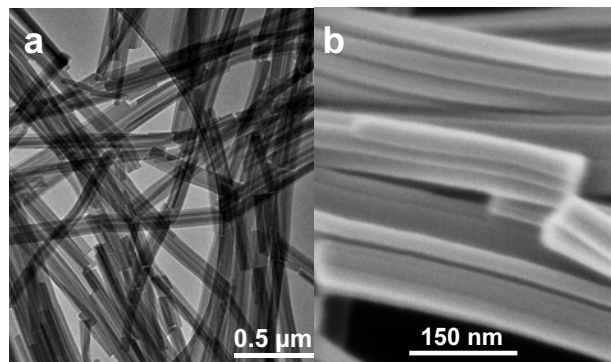


Fig. 9 shows microscale tubules formed from two porphyrin tectons, again with *SnTPPS*<sub>4</sub> and a free base porphyrin as the ionic tectons. However, in this case an amino acid is also present and may be incorporated into the microtubes. The microtubes are flexible, have thin walls that tend to collapse when dried, and tend to grow like ‘fur’ from the glass surface of the vessel in which they form over a period of days after mixing.

Fig. 10 show nanofiber bundles formed by ionic self-assembly in a two-phase solvent system where one porphyrin is dissolved in water and the other is dissolved in an organic solvent ( $\text{CH}_2\text{Cl}_2$ ).<sup>14</sup> Phase-transfer of the water-soluble porphyrin to the organic phase generates the porphyrin nanofiber bundles by ionic self-assembly. Our discovery that porphyrin

nanostructure can be made by phase-transfer ionic self-assembly is important because most synthetic porphyrins are not soluble in water. The isolation of new porphyrin nanomaterials with different structural and optical characteristics than the previously described nanotubes indicates that ionic self-assembly is a general method for making novel functional porphyrin-based nanomaterials.



**Fig. 10.** Electron microscopy of the porphyrin nanofiber bundles: (a) TEM image; (b) SEM image.

The molecular structures of the porphyrin tectons used to make the nanofiber bundles are shown in the inset of Fig. 11. An Sb(V) complex was chosen because Sb(V) porphyrins are known to be good reductive photocatalysts in homogeneous solutions, and thus might allow the production of metal composite nanostructures. In a typical reaction, 9 mL of a 105 μM aqueous solution of 5,10,15,20-tetrakis(4-sulfonatophenyl)-porphyrin,  $[\text{H}_2\text{TPPS}_4]^{4-}$  was added to 9 mL of a 315 μM dichloromethane solution of the oxo-Sb(V) complex of 5,10,15,20-tetraphenylporphyrin,  $[\text{Sb}(\text{V})\text{OTPP}]^+$  in a 20-mL glass vial. This two-

phase system was shaken vigorously for 2 minutes, followed by vigorous stirring with a magnetic stirrer bar for 1 hour. The liquid/liquid interface re-established shortly after agitation was stopped, and about 1 hour later strands of a pink material appeared in the organic phase. This material tended to float up to the interface but could be re-dispersed in the dichloromethane by gentle swirling. Transmission electron microscopy images (Fig. 10a) show that the pink material is composed of rod-like nanostructures, which are reasonably uniform in size and shape and approximately 70-130 nm wide and 1-2 μm long. High-resolution scanning electron microscopy images reveal that each 'rod' actually consists of a bundle of fibers that are 20-40 nm in diameter (Figs. 10b). If the liquid-liquid interface was not disturbed during the synthesis, micron-sized rods with a wide distribution of widths and lengths were obtained (not shown).

The molar ratio of  $[\text{Sb}(\text{V})\text{OTPP}]^+$  to  $[\text{H}_2\text{TPPS}_4]^{4-}$  in the nanofiber bundles was measured by elemental microanalysis, UV-visible absorption spectroscopy, and Energy Dispersive X-ray spectroscopy (EDX). A ratio of 3.7:1 was obtained by elemental analysis, which is consistent with the less accurate determinations from EDX and from simulation of absorption spectra. The ratio is close to the ratio of 4:1 expected from the charges of the individual ionic tectons, and is consistent with the formation of an ionic solid from the porphyrin tectons without the participation of other ions. Additional studies showed that a range of porphyrins could be incorporated into the nanofiber bundles, allowing fine tuning of their physicochemical properties. For example, nanostructures with similar morphologies were obtained with a range of complexes of  $[\text{H}_2\text{TPPS}_4]^{4-}$  containing divalent metals such as Cu, Ni, Ag, and Zn.

The optical properties of the nanofiber bundles are quite different from those reported by us for the porphyrin nanotubes. The UV-visible spectrum of the nanotubes shows intense red-shifted bands indicative of a *J*-aggregate structure, and the fluorescence of the porphyrins in the nanotubes is also quenched. In contrast, the UV-visible absorption spectrum of the bundled nanofibers dispersed in dichloromethane shows several Soret bands that might originate from porphyrins in monomer-like

and aggregated states (Fig. 11). For example, the bands at 422 nm, 516 nm, 560 nm and 598 nm are likely due to monomeric species. One Soret band at 394 nm is blue-shifted compared to the monomeric species, whereas another band at 450 nm is red-shifted; these features may suggest the presence of *H*- and *J*-type aggregate structures, respectively. In addition, the porphyrin nanofiber bundles are highly fluorescent and emit intense red light when excited with blue light (as shown by the confocal fluorescence image in Fig. 11).

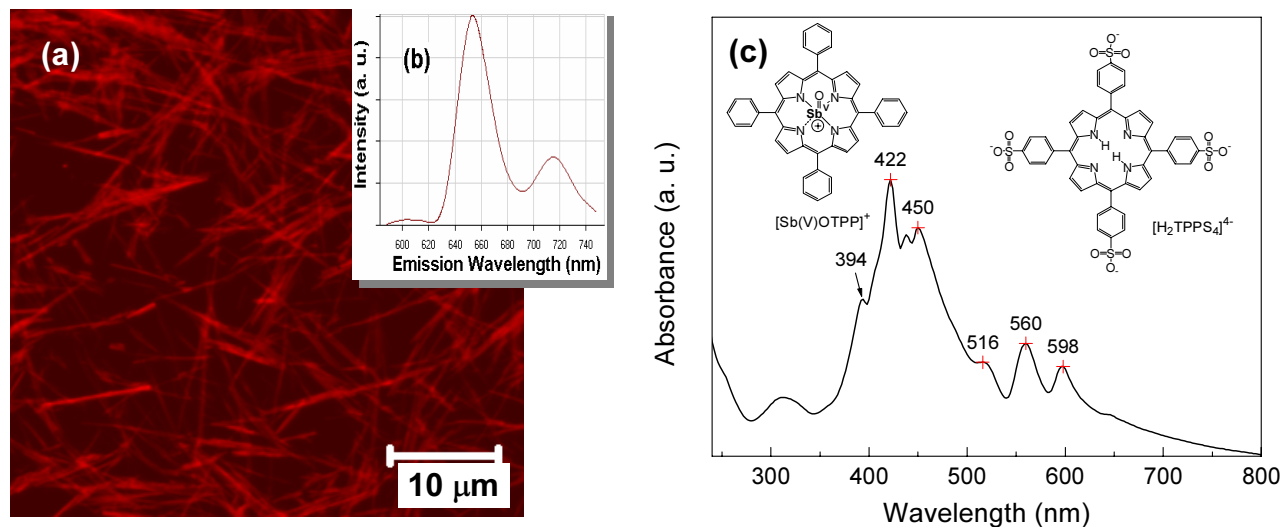


**Fig. 11.** Confocal fluorescence micrograph of the porphyrin nanofiber bundles (a), and representative emission spectrum (b) from one spot on an individual bundle (excitation laser line: 488 nm). Right panel: UV-visible spectrum of the porphyrin nanofiber bundles dispersed in  $\text{CH}_2\text{Cl}_2$  and the molecular structures of the porphyrin tectons.

The emission spectrum from a single spot on an individual bundle was obtained (Fig. 11), and shows three peaks at 603 nm, 653 nm, and 715 nm. The bands at 603 and 715 nm can be assigned to  $[\text{Sb}(\text{V})\text{OTPP}]^+$  and  $[\text{H}_2\text{TPPS}_4]^{4+}$ , respectively, while the band at 653 nm contains contributions from both porphyrins. The ratio of the intensities of the bands at 603 nm and 715 nm is about 0.1, which is much smaller than the ratio of 0.5 obtained from a simulation based on the fluorescence spectra of monomeric  $[\text{Sb}(\text{V})\text{OTPP}]^+$  and  $[\text{H}_2\text{TPPS}_4]^{4+}$  (not shown). This may indicate that energy transfer from  $[\text{Sb}(\text{V})\text{OTPP}]^+$  to  $[\text{H}_2\text{TPPS}_4]^{4+}$  is occurring when the bundles are photoexcited.

Summarizing, we have succeeded in extending the synthesis of porphyrin nanostructures by ionic self-assembly to a two-phase system allowing the use of a large library of water insoluble porphyrin tectons. Using this phase-transfer method, we have prepared these bundles of porphyrin nanofibers, which have different optical properties from the previously reported porphyrin nanotubes. The porphyrin nanofibers may find applications as nanoscale devices in electronics, photonics, fluorescence sensing, and solar energy conversion and storage, and will also be easier to work with under aqueous conditions.

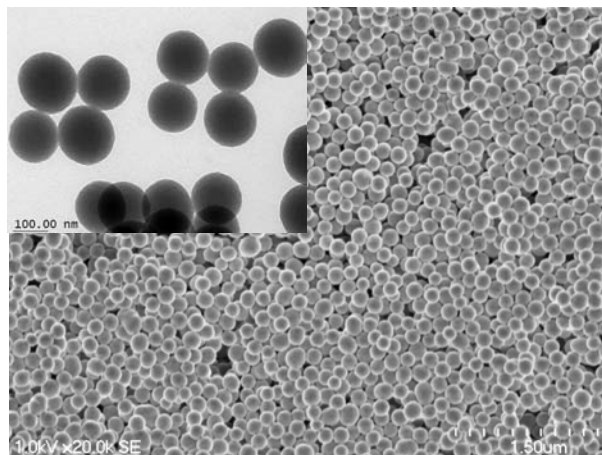


**Fig. 12.** SEM images of solid porphyrin nanospheres formed by metal complex formation-induced self-assembly of a tin porphyrin. Inset: TEM image of the nanospheres.

Fig. 12 shows our most recent discovery in the research area, namely porphyrin spheres, which are self-assembled by coordination of pyridyl groups of SnTPyP to a metal complex. Coordination of the pyridine groups to the metal complex causes the porphyrins to crosslink between porphyrins, leading to the uniform-sized solid spheres shown in the TEM and SEM images of Fig. 12. The average diameter of the porphyrin spheres is about 120 nm. The nanospheres are stable structures between pH 2 and 12.

Array-based CB sensing has emerged as a powerful approach for the detection of chemically diverse analytes. Based on cross-responsive sensor elements, rather than receptors for specific species, these systems produce unique composite responses, in a fashion similar to the olfactory system. Colorimetric array detection (so-called ‘smell-seeing’) of a wide range of agents has been achieved using a family of porphyrins immobilized on silica gel.<sup>3</sup> Color change patterns obtained from the array give visual identification of a range of chemicals (*e.g.*, alcohols, amines, ethers, phosphines, phosphites, thioethers, thiols, arenes, halocarbons, ketones). Diffuse reflectance spectroscopy is used to reveal the solid-state color changes, providing good linear responses and limits of detection (ppb). Resonance light scattering and fluorescence offer some advantages detection by optical absorption because of the intensity of the emission. We have evaluated the potential for arrays of porphyrin nanotubes and other porphyrin nanostructures as sensing elements for fabricating CB microsensors. The use of arrays of nanoscale sensing elements like the porphyrin nanotubes offer unique opportunities for ultrasensitive detection approaching single molecule limits.



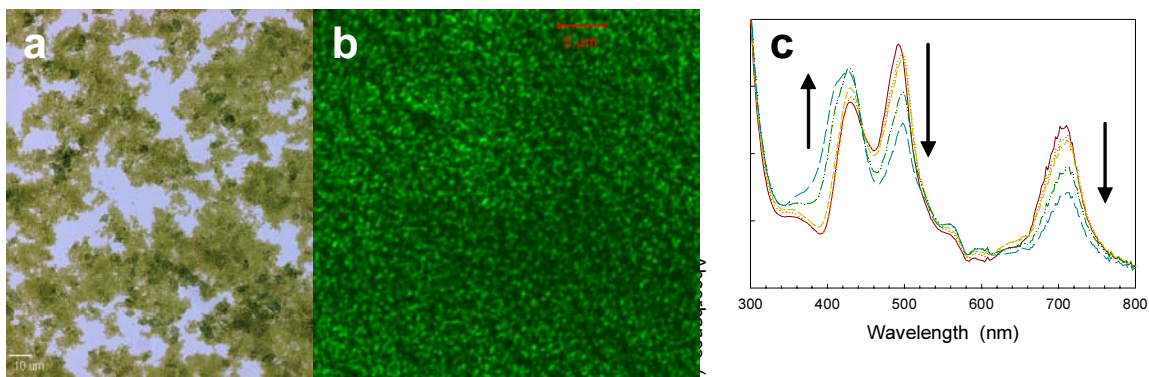


**Fig. 13.** Normal (a) and higher magnification confocal (b) microscope images of solid porphyrin nanotubes deposited on glass substrate. Confocal image is in the green resonance scattered light from the nanotubes. Absorption/resonance light scattering changes as a function of pyridine concentration in air.

Fig. 13 shows microscope images of a film of porphyrin nanotubes deposited on a glass. The width of the individual nanotubes is too small to be resolved even in the confocal microscope image obtained in resonance scattered light from green laser excitation. The normal white light micrograph shows that many regions are not covered by the tubes. The porphyrin-nanotube films on microscope glass slides are made by drop-casting of the porphyrin-nanotube aqueous suspension. A similar technique is used to make sensor systems for the determination of the optical response of the nanotubes to gas-phase chemicals, as illustrated for pyridine in Fig. 13c.

For these optical response measurements, the glass slide coated with porphyrin nanotubes was put into a sealable 1-cm pathlength quartz glass cuvette. The UV-visible spectrum was obtained in air before analyte exposure, then the nanotubes were exposed to pyridine or acetic acid by adding a small amount of the neat liquid in a capillary tube inserted in the cuvette. The UV-visible spectra of the slide were taken at 15 s, 60 s, and 180 s after exposure to the solvent vapor in the sealed cuvette. The capillary tube was then taken out, and the nanotube film was exposed to air in the cuvette for 15 minutes and a final spectrum of the slide was measured. The spectral changes observed for pyridine and acetic acid exposures occur in opposite senses (see arrows in Fig. 13c) but are broadly similar. This suggests that the spectrum of the nanotubes is sensitive to slight pH variations caused by the adsorbed acid (acetic acid) or base (pyridine). This interpretation is consistent with the known extreme pH sensitivity of the tube structure. This was confirmed by exposing the porphyrin nanotube film to other acids and bases (*e.g.*,  $\text{NO}_2$ ), which caused spectral changes similar to acetic acid and pyridine, respectively.

In summary, we have clearly demonstrated that many porphyrin nanostructures can be made and that their morphologies and properties are subject to synthetic manipulation. These porphyrin nanostructures provide a new way of incorporating responsive materials into integrated nanosystems, using bio-inspired strategies for developing and assembling the desired materials and systems. While we have gained some control over the structures and properties of these new nanostructures, it is clear that a good deal more work is required to fully understand the self-assembly processes that lead to these unique nanomaterials. We have also provided preliminary evidence that the porphyrin-based nanostructures function in ways that might allow the integration of these functional components into microelectronics to produce devices such as CB sensors. We expect the porphyrin nanotubes and the other porphyrin nanostructures we have discovered in this work may have many potential uses in microelectronics and photonics applications.



## References:

1. Wang, Z.; Medforth, C. J.; Shelnutt, J. A., *J. Am. Chem. Soc.* **2004**, *126*, 15954-15955.
2. Wang, Z.; Medforth, C. J.; Shelnutt, J. A., *J. Am. Chem. Soc.* **2004**, *126*, 16720-16721.
3. Suslick, K. S., *et al.*, In *Artificial chemical sensing: olfaction and the electronic nose*; Stetter, J. R. and Penrose, W. R., Ed.; Electrochemical Society: Pennington, NJ, 2001, pp 8-14.
4. Whitesides, G. M., *et al. Acc. Chem. Res.* **1995**, *28*, 37.
5. Cao, L., *et al. Advanced Materials* **2003**, *15*, 909-913.
6. Cao, L., *et al. Chem. Mater.* **2003**, *15*, 3247-3249.
7. Siggel, U., *et al. Ber. Bunsen-Ges. Phys. Chem.* **1996**, *100*, 2070-2075.
8. Yamaguchi, T., *et al. J. Am. Chem. Soc.* **2003**, *125*, 13934-13935.
9. Schwab, A. D., *et al. J. Phys. Chem. B* **2003**, *107*, 11339-11345.
10. Rotomskis, R., *et al. J. Phys. Chem. B* **2004**, *108*, 1833-2838.
11. Marks, T. J. *Science* 1985, *227*, 881-889.
12. van Rossum, V.-J., *et al. Biochemistry* **2001**, *40*, 1587-1595.
13. Song, Y., *et al., J. Am. Chem. Soc.* **2004**, *126*, 635-645.
14. Wang, Z.; Medforth, C. J.; Shelnutt, J. A., *J. Am. Chem. Soc.* **2005**, *submitted.*

**Distribution:**

1	MS 0123	LDRD Donna Chavez, 1011
10	MS 1349	John A. Shelnut, 1114
1	MS 1415	Carlos Gutierrez, 1114
2	MS 9018	Central Technical Files, 8945-1
2	MS 0899	Technical Library, 9616



**Sandia National Laboratories**